ELSEVIER

Chemical Engineering Science 61 (2006) 5934–5943

Chemical Engineering Science

www.elsevier.com/locate/ces

Effective diffusivities and pore-transport characteristics of washcoated ceramic monolith for automotive catalytic converter

Tomáš Starý[a], Olga Šolcová[b,*], Petr Schneider[b], Miloš Marek[a]

[a]*Department of Chemical Engineering, Institute of Chemical Technology, Prague, Technická 5, 166 28 Prague 6-Dejvice, Czech Republic*
[b]*Institute of Chemical Processes Fundamentals, Academy of Science of the Czech Republic, Rozvojová 135, 165 02 Prague 6-Suchdol, Czech Republic*

Received 27 April 2006; accepted 9 May 2006
Available online 19 May 2006

Abstract

Using the chromatographic technique (carrier-gas: N_2; tracer-gases: He, Ar) the effective diffusivity in single-pellet string columns (SPSC) packed with porous slab particles was studied. Dispersion due to extra-column effects was eliminated via convolution of column responses for two lengths. The measurements were done for cordierite particles and for cordierite coated with alumina-based washcoat. The effective diffusion coefficients for two tracer–carrier pairs were evaluated by fitting column response (chromatographic) peaks in time-domain. Mean transport parameters were evaluated for both types of porous particles. The obtained mean transport pore radii are in reasonable agreement with pore-size distribution from mercury porosimetry.

Keywords: Single-pellet string column (SPSC); Diffusion; Mass transfer; Transport processes; Parameter identification; Catalyst monolith

1. Introduction

Structured catalyst supports are widely used in automotive exhaust gas converters. Small sized channels are contained in monoliths to provide large surface area. Typically, both metal and ceramic monoliths are used (Cybulski and Moujin, 1998; Kašpar et al., 2003). Ceramic monoliths made from cordierite with square channels are employed quite extensively because of relatively low production costs (Gulati, 1998; Heck and Farrauto, 1995). The active catalyst is supported (washcoated) onto the monolith by dipping it into slurry containing the catalyst precursors. A commonly used washcoat material is γ-Al_2O_3 with a surface area of 100–200 m^2/g. The excess of the deposited material (washcoat) is then blown out with hot air and monolith is calcined to obtain the catalyst (Kašpar et al., 2003; Heck and Farrauto, 1995; Twigg and Wilkins, 1998). This process gives a thin washcoat layer; however, it also results in a variation in washcoat layer thickness around the channel perimeter. Although the washcoat layer is thin, pore diffusion can affect monolith performance (Kočí et al., 2004; West et al., 2003; Mukadi and Hayes, 2002; Leung et al., 1996; Ramathan et al., 2003), and, thus, need to be included in any realistic mathematical model. Therefore, it is necessary to have reliable information on the mass transport rate in the porous medium (e.g., effective diffusivities of exhaust gases in the washcoat layer).

Several techniques for obtaining pore-transport characteristics in washcoat layer have been used (Kolaczkowski, 2003). One approach is based on the Wicke–Kallenbach counter-current diffusion cell; here sections of a washcoated monolith are used (Zhang et al., 2004), which allows diffusion normal to the direction of the gas flow. Beeckman's (1991) approach is suitable for larger diameters of monolith channel (2 mm and larger). A block of seven channels cut from the monolith is mounted into the diffusion cell. From the substance balance the effective diffusivity can be calculated (Kolaczkowski, 2000).

An approach inspired by the chromatographic method is described in this paper. The chromatographic method for evaluation of effective diffusion coefficients in porous materials is well established (Schneider and Smith, 1968a,b; Haynes, 1988). Porous particles can be packed into the column in two

* Corresponding author. Tel.: +42 0296780279; fax: +42 0220920661.
E-mail address: solcova@icpf.cas.cz (O. Šolcová).

0009-2509/$ - see front matter © 2006 Elsevier Ltd. All rights reserved.
doi:10.1016/j.ces.2006.05.014

ways: either a wide bed is packed with particles (with column/particle diameter ratio larger then 20) or in an arrangement known as single-pellet string column (SPSC) (Scott et al., 1974). In SPSC, particles are packed one by one into a column with diameter that exceeds only slightly (10–20%) the particle dimension. SPSC is usually used for spherical or cylindrical porous particles (Šolcová et al., 1997; Šolcová and Schneider, 2004) and could be also used for porous solids with other shapes (Šolcová et al., 2006). Monoliths with 400 cells per square inch, which corresponds to channels internal dimension approximately 1 mm, were used in this study.

Effective diffusivities are evaluated from response (chromatographic) signals of columns packed with particles of the tested porous material. A pulse of tracer gas (T) is injected into the carrier-gas (C) stream, which flows at constant flow rate through the column. The tracer concentration is measured at the column outlet by a detector. The recorded outlet response signal is then analyzed. Analysis of outlet peaks is based on the transport processes inside the column. The transport model by Kubín–Kučera (Kubín, 1965; Kučera, 1965) has been used nearly exclusively. Matching of column response peaks with model equations was usually done via the response moments (Schneider and Smith, 1968a,b; Guasguo et al., 2000). Nowadays, it is possible to perform the matching in the time-domain (Fahim and Wakao, 1982; Wakao et al., 1979; Schneider, 1984). The Kubín–Kučera model describes intracolumn processes, such as convection and axial dispersion of the tracer band, transport of the tracer through a laminar film around the packing particles, diffusion in the pore structure and adsorption (for adsorbable tracer gas) on the internal surface of porous packing. But it does not account for processes upstream and downstream of the column (extra-column effects). It has been suggested (Šolcová and Schneider, 1996) that these processes could be included in the time-domain matching through application of the convolution theorem. This requires experimental system responses for two different lengths of columns.

In the general case parameter determination by time-domain matching requires simultaneous search for five parameters. In such case the parameter confidence is very low. To increase the confidence we have used non-adsorbable gases and worked with higher carrier-gas velocities. This prevents adsorption, resistance due to transport through the laminar film and the possible surface diffusion, which obscures the obtained effective diffusivities and transport characteristics. It was also shown that Peclet numbers (which characterize axial dispersion) determined for SPSC with non-porous packing could be used in matching the responses of porous packing (Šolcová and Schneider, 2004). For SPSC with porous particles this decreases the number of fitted parameters and removes part of the undesirable parameter correlation.

It is the aim of this work to evaluate effective diffusion coefficients for different tracer→carrier pairs and to find consistent transport characteristics of the washcoat layer. These characteristics are independent of temperature and pressure, as well as the nature of gases that are transported through pores and permit calculation of effective diffusivities for any gas pair at other conditions.

2. Experimental

2.1. Samples

The tested particles were cut from a commercial ceramic catalytic converter monolith with 400 cells per square inch. Two systems were chosen for this study: the blank ceramic support (S) and the washcoat (W) coated monolith three-way catalyst ($W\&S$). Each packing particle had a cubic shape with dimensions $4.3 \times 5.9 \times 3$ mm. The square shape of the cells for the blank ceramic support monolith and the variation of the washcoat thickness around the perimeter when the monolith is coated by the washcoat can be recognized in Fig. 1. Thicker washcoat layers appear in the corners of the cells. The average thickness of the washcoat layer was determined from the analysis of a number of cells. The wall thickness of the blank ceramic support varied around 140 μm and for the coated monolith the total thickness of washcoat and support varied around 210 μm.

Textural properties of tested samples were determined by the mercury porozimetry (AutoPore9200, Micromeritics, USA), the helium pycnometry (Accupyc1320, Micromeritics, USA) and by the physisorption of nitrogen (ASAP2010M, Micromeritics, USA). The pore-size distributions are shown in Fig. 2. It is clearly seen that the ceramic support has bidisperse structure with the most frequent pore radii around 1 and 3 μm. The monolith with the deposited washcoat shows the combined influence of the support and washcoat. $W\&S$ sample has a tridispersed structure. Two peaks with pore radii around 200 nm and 1 μm come from the ceramic support and are shifted to narrow pores of coating washcoat. The third peak around 5 nm belongs to the washcoat layer. Other

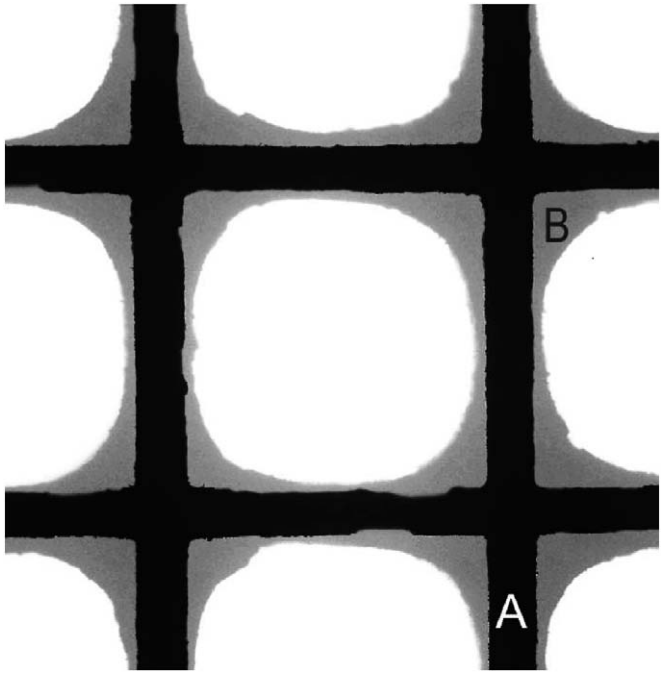

Fig. 1. Monolith channels: (A) ceramic support and (B) washcoat layer on the ceramic support.

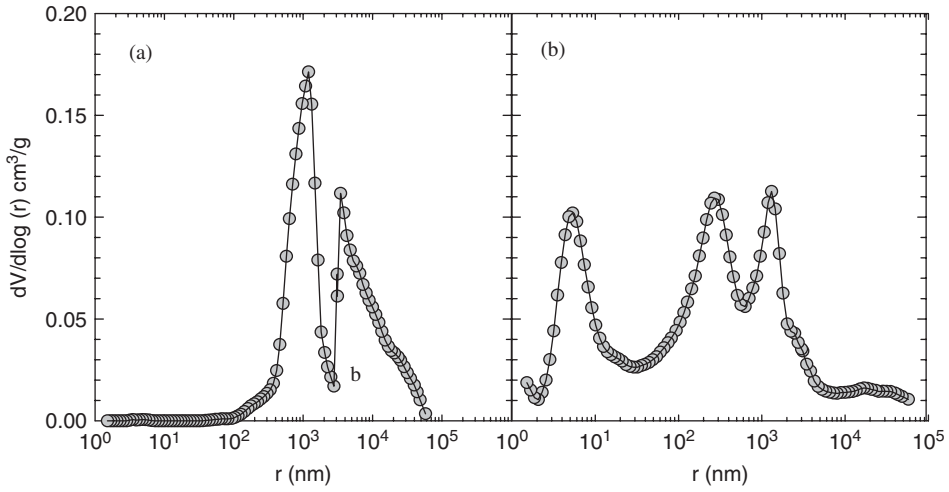

Fig. 2. Pore-size distribution: (a) ceramic support (*S*) and (b) washcoat on ceramic support (*W&S*).

Table 1
Textural properties

	Washcoat on support *W&S*	Ceramic support *S*
Surface area (m^2/g)	14.72	0.16
Pellet density, ρ_p (g/cm^3)	1.55	1.60
Skeletal density, ρ (g/cm^3)	3.06	2.53
Pore volume, V_p (cm^3/g)	0.21	0.15
Particle porosity, β (dimensionless)	0.33	0.23
Total pore volume (ml/g)	0.21	0.15

Table 2
Variation in skeletal density

Sample number	Skeletal density (g/cm^3)
1	3.03
2	2.95
3	3.08
4	3.17
5	2.94
6	3.14
7	2.95
8	3.20
9	3.22
10	2.90

textural properties are summarized in Table 1. For the true density of *W&S* the average value obtained from measurements of eight various *W&S* pieces was used. Skeletal density changed from sample to sample depending on the position around the perimeter of the monolith. This is in agreement with fact that the distribution of the washcoat is not uniform around the monolith perimeter. No variations in the skeletal densities for ceramic support were observed. Variations in true density of *W&S* samples are summarized in Table 2.

2.2. Experimental setup

The chromatographic system consisted of calibrated mass flow-meter/controllers for carrier and tracer gases, a six-way sampling valve for tracer gas with sampling loop (0.273 cm^3), chromatographic column (SPSC) and thermal conductivity detector (TCD). Metal capillaries, with 1 mm inner diameter, were employed for connecting the system components. Two columns with lengths $L_I = 100$ cm and $L_{II} = 50$ cm and identical column diameters (8 mm) were packed in identical manner either with the ceramic support (*S*) or ceramic support with washcoat layer (*W&S*). In addition, columns packed with *S* and *W&S*

Table 3
Column and packing characteristics

Column length (cm)	100		50	
Column inner diameter (cm)	0.8		0.8	
Cross-section area (cm^2)	0.5027		0.5027	
	Washcoat on support *W&S*		Ceramic support *S*	
	L_I	L_{II}	L_I	L_{II}
Column void fraction, α[a] (dimensionless)	0.794		0.886	
Column void fraction, α[b] (dimensionless)	0.819	0.818	0.884	0.871
Packing weight—porous (g)	14.194	7.054	10.311	4.614
Packing weight—non-porous (g)	20.142	9.262	12.063	5.292
Number of particles—porous	270	135	268	138
Number of particles—non-porous	268	137	266	126

[a]From moment theory.
[b]From Eq. (12).

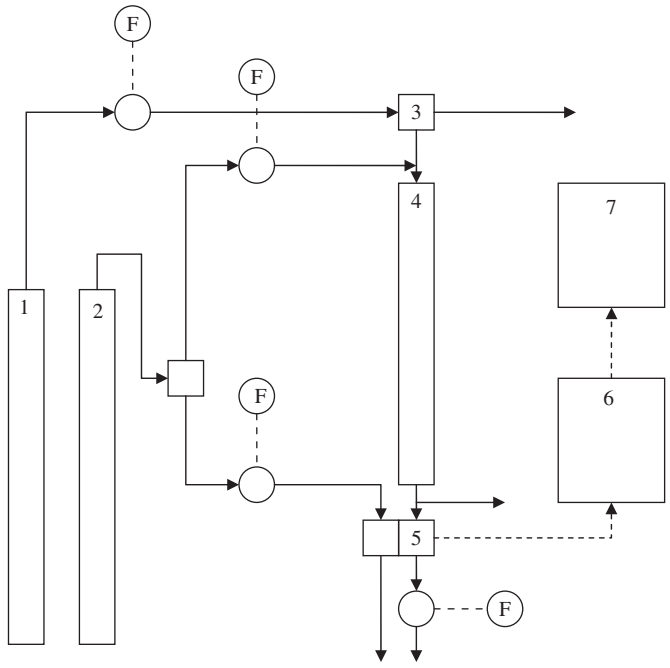

Fig. 3. Chromatographic setup: (1) tracer-gas source, (2) carrier-gas source, (3) sampling valve, (4) chromatographic column, (5) thermal conductivity detector (TCD), (6) digital data logger, (7) computer, and (F) calibrated mass flow-meter/controllers.

soaked by Porofil (Beckman–Coulter, USA) were used to obtain information on axial dispersion. According to the manufacturer $\sigma \cos\theta = 0.16$ bar μm (where σ is the Porofil surface tension, and θ the contact angle). From comparison of capillary outflow-time for water and Porofil its viscosity was estimated as $\mu = 1.25$ mPa s. Information about the number of packed particles into each SPSC system as well as the basic column dimensions are summarized in Table 3. The whole setup is depicted in Fig. 3.

2.3. Column responses

All measurements were made at laboratory temperature and pressure. Signals from the TCD were recorded in a digital data logger (1000 data points). After zero-line correction (less than 0.1% of the maximum response height) about 80 uniformly distributed points, normalized to the maximum tracer concentration, were retained for further processing. Because the system responses were quite rapid the positions of maxima of replicated peaks differed slightly (0.1–0.2 s). Therefore, the mean maximum position was determined and the replicated peaks were shifted to this maximum. The final response peak was, then, obtained by averaging the individual responses. Three responses were obtained for every carrier-flow rate and carrier–tracer pair of gases.

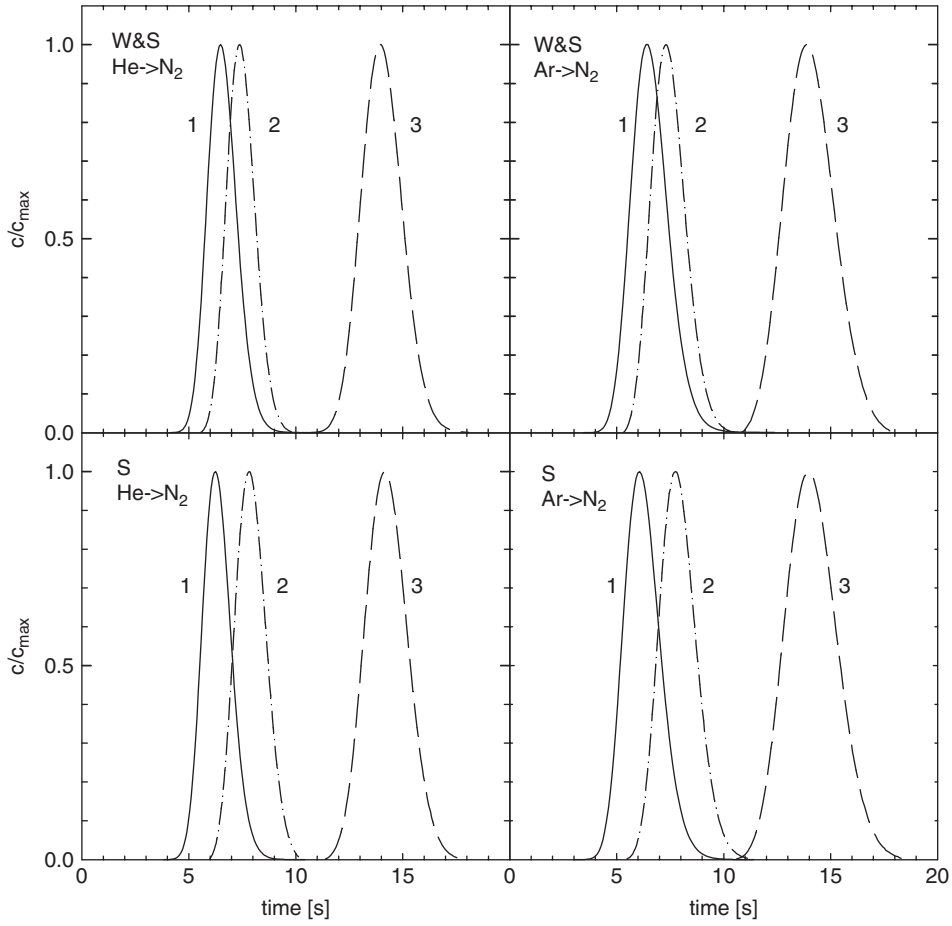

Fig. 4. Response peaks for both column lengths, *W&S* and *S*: (1) response of shorter column dash-dot line, (2) impulse response—solid line, and (3) response of longer column—dotted line.

Nitrogen was used as carrier and helium and argon as tracers (denoted as He → N_2 and Ar → N_2). Nitrogen volumetric flow rates varied between 30 and 200 cm^3/min and tracer was delivered via the sample loop (0.273 cm^3 volume).

As an illustration Fig. 4 shows responses for both *W&S* and *S* column lengths and the same linear carrier-gas velocity together with the impulse response for the optimum parameter set t_c, Pe, t_{diff}, γ/β and δ_0. Because the difference between the lengths of columns I and II ($L_c = 50$ cm) is the same as the length of the shorter column II, L_{II}, the difference between the position of peak 3 (impulse response) and peak 2 (shorter column) corresponds to extra-column effects. Obviously, the neglection of these effects would significantly bias the obtained t_c, Pe, t_{diff}, γ/β and δ_0 parameters.

3. Theoretical

3.1. Tracer impulse response of the chromatographic system

The chromatographic column (length L) is packed with infinite porous slabs with half-thickness ℓ and porosity β. Carrier gas, C, flows with constant interstitial linear velocity, v. The column void fraction (per unit column volume) equals α. A Dirac impulse of tracer gas, T, is introduced at the column inlet. If tracer-gas convection and axial dispersion is taken into account the tracer mass balance in the interparticle space (per unit volume of interparticle spaces) can be expressed as

$$\frac{1}{Pe}\cdot\frac{\partial^2 c}{\partial x^2}-\frac{\partial c}{\partial x}-t_c\cdot\frac{\partial c}{\partial t}-\frac{t_c}{t_{diff}}\cdot\frac{\gamma}{\beta}\ell\left.\frac{\partial u}{\partial r}\right|_{r=\ell}=0 \tag{1}$$

with tracer concentration in the interparticle space, $c(x,t)$ and the dimensionless column length coordinate x ($x \in (0,1)$); $\gamma/\beta = (1-\alpha)/\alpha$ with α the column void fraction α; $u(x,r,t)$ is the tracer concentration in pores. The convection, t_c, and diffusion, t_{diff}, times are defined as $t_c = L/v$; $t_{diff} = \ell^2/D_{TC}$ and D_{TC} denotes the effective diffusion coefficient of the pair $T \rightarrow C$. The pellet length coordinate r ($r \in (0,\ell)$) starts at the pellet center plane ($r = 0$). The Peclet number, Pe, is based on column length $Pe = vL/E$. Tracer concentration in the interparticle space at the column inlet is $c(0,t) = \delta(t)$, where $\delta(t)$ denotes the Dirac impulse of tracer.

With the tracer pore concentration $u(r,x,t)$ and concentration of adsorbed tracer $w(r,x,t)$ the tracer balance in the unit pellet volume reads

$$D_{TC}\frac{\partial^2 u}{\partial r^2}-\beta\frac{\partial u}{\partial t}-\rho\frac{\partial w}{\partial t}=0. \tag{2}$$

For tracer equilibrium adsorption with linear adsorption isotherm (with dimensionless tracer adsorption equilibrium constant, K), $w = (\beta/\rho)Ku$ and balance (2) has the form

$$D_{TC}\frac{\partial^2 u}{\partial r^2}-\beta(1+K)\frac{\partial u}{\partial t}=0 \tag{3}$$

with boundary condition for the centre of the porous slab $(\partial u/\partial r)|_{r=0} = 0$ and the outer pellet surface ($r = \ell$) $c(x,t) = u(\ell,x,t)$.

System of PDEs (1) and (3) can be solved by Laplace transformation to yield the Laplace image of the *column impulse response* $C(1,s)$

$$C(1,s) = C_0(s)\exp\left[\frac{Pe}{2}(1-\sqrt{H(s)})\right], \tag{4}$$

$$H(s) = 1+\frac{4t_c}{Pe}[s+\kappa(s)], \tag{5}$$

$$\kappa(s) = \frac{\gamma/\beta}{t_{diff}}M\tanh(M), \tag{6}$$

$$M(s) = \sqrt{\frac{s\delta_0 t_{diff}}{\gamma/\beta}}. \tag{7}$$

For a given set of parameters t_c, Pe, t_{diff}, γ/β and δ_0 points of the column impulse response $c(x=1,t)$ were obtained by numerical inversion of the complex Laplace form (4) by De Hoog algorithm (Honig and Hirdes, 1984; Seidel-Morgenstern, 1991) with complex variables.

3.2. Analysis of chromatographic peaks

To remove the extra-column effects (due to, e.g., connection tubing, sampling valve, TCD, column inlet and outlet, etc.) responses for two columns, I and II (lengths L_I and L_{II}, $L_I > L_{II}$), can be used together with the convolution theorem. It follows that the column response, $c(t)$, is given by

$$c(t) = \int_0^t g(t-u)h(u)\,du, \tag{8}$$

where $g(t)$ describes the shape of the signal entering the column instead of the Dirac pulse. In linear systems it is immaterial if the extra-column effects are distributed in different locations of the system or if they are concentrated in one position and in what order they are arranged. Therefore, the experimental response for the shorter column II (length L_{II}) can be used in place of $g(t)$, and the impulse response, $h(t)$, for column of length $L_c = L_I - L_{II}$ is evaluated by numerical inversion of the Laplace transform of impulse response (4).

For a given set of parameters, t_c, Pe, t_{diff}, γ/β and δ_0, integrals (8) were evaluated numerically with the Romberg algorithm (Press et al., 1986). The short column responses were interpolated by the cubic spline method. The simplex algorithm (Press et al., 1986) then performed search for optimum t_c, Pe, t_{diff}, γ/β and δ_0 parameters with the sum of squared deviations between experimental and calculated long column (II) responses as objective function. The obtained parameters, t_c, Pe, t_{diff}, γ/β and δ_0, correspond to column length $L_c = L_I - L_{II}$.

4. Results and discussion

4.1. Column parameters

In order to decrease the number of fitted parameters and, thus, to increase the parameters confidence, parameters γ/β and δ_0 were evaluated independently.

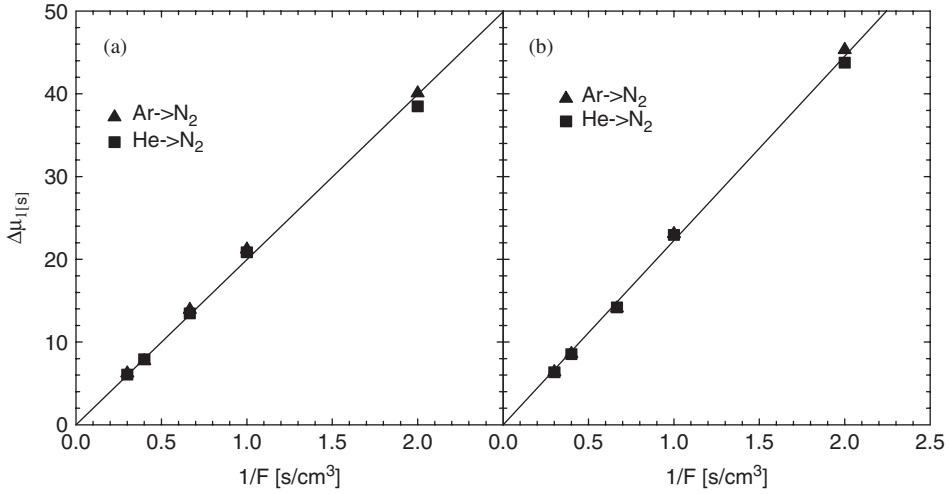

Fig. 5. $\Delta\mu_1'$ versus $1/F$ for particles with pores blocked by Porofil: (a) *W&S* and (b) *S*.

The *column void fraction*, α, can be obtained in two ways:

(i) from the difference of first absolute peak moments, $\Delta\mu_1 = (\mu_1)_{\mathrm{I}} - (\mu_1)_{\mathrm{II}}$, of column responses for columns I and II packed with ceramic support (*S*), and the washcoated support (*W&S*), with pores blocked by Porofil. In this case the column packing is non-porous ($\beta = 0$) and the difference of first absolute moments of response peaks equals (Schneider and Smith, 1968a,b)

$$\Delta\mu_1' = t_c, \tag{9}$$

with the mean residence time, t_c,

$$t_c = L/v, \tag{10}$$

where v is the linear interstitial tracer velocity

$$v = F/A\alpha \tag{11}$$

and F is the volumetric carrier-gas velocity and A is the column cross-section. Fig. 5 shows the dependence $\Delta\mu_1'$ versus $1/F$ for Ar $\rightarrow$ N_2 and He $\rightarrow$ N_2 tracer–carrier pairs for columns packed with *W&S* and *S* particles with Porofil blocked pores. Void fractions α_{WS} (washcoat and support) and α_S (support) obtained from the identical slopes for both $T \rightarrow C$ pairs are shown in Table 3.

(ii) From the knowledge of packing weight for each column and mercury densities for both types of particles. Column void fraction, α, was then evaluated from

$$\alpha = \left(V_{\mathrm{column}} - \frac{m_{\mathrm{packing}}}{\rho_{\mathrm{Hg,packing}}} \right) \Big/ V_{\mathrm{column}}. \tag{12}$$

The obtained void fractions for columns packed with the support, α_S, and the coated support, α_{WS}, are shown in Table 3. Averaged values were used in further calculations.

Parameters γ/β *and* δ_0 follow from the dependence $\Delta\mu_1'$ versus t_c for columns I and II packed with (dry) *W&S* and *S*. In this case $\beta \neq 0$ and

$$\Delta\mu_1' = t_c(1 + \delta_0), \tag{13}$$

$$\gamma/\beta = \frac{1-\alpha}{\alpha}. \tag{14}$$

As both tracer and carrier gases are not adsorbed on the packing, adsorption equilibrium constants $K_T = 0$ and $\gamma = \delta_0$.

Peclet numbers, *Pe*, for both $T \rightarrow C$ pairs and columns with *W&S* and *S* packing, were evaluated from responses of column packed with pore-blocked packings in two ways:

(i) from differences of second central and first absolute moments of response peak from columns with pore-blocked packing and
(ii) by time-domain matching of response peak from the same columns.

Moment analysis: The difference of the second central moments of the response peaks equals

$$\Delta\mu_2 = \frac{2t_c^2}{Pe}. \tag{15}$$

From expressions (9) and (15) for moments $\Delta\mu_2$ and $\Delta\mu_1'$ it follows that

$$Pe = 2\frac{(\Delta\mu_1')^2}{\Delta\mu_2}. \tag{16}$$

Peclet numbers for different $T \rightarrow C$ pairs and columns with both kinds of packing with blocked pores evaluated from (16) are shown in Fig. 6. The product of Reynolds and Schmidt numbers, *ReSc*, is used as the independent variable.

Time-domain response peak fitting, for columns packed with pore-blocked packings, was performed according to the convolution integral (8). The Dirac impulse response, $h(t)$, for the axially dispersed plug-flow is known explicitly (Himmelblau and Bischoff, 1968):

$$h(t) = \frac{1}{t_c}\sqrt{\frac{Pe\,t_c}{4\pi t}}\exp\left[-\frac{Pe\,t_c}{4t}\left(1-\frac{t}{t_c}\right)^2\right]. \tag{17}$$

Hence, two parameters (the tracer mean-residence time, t_c, and Peclet number, *Pe*) are determined during time-domain fitting.

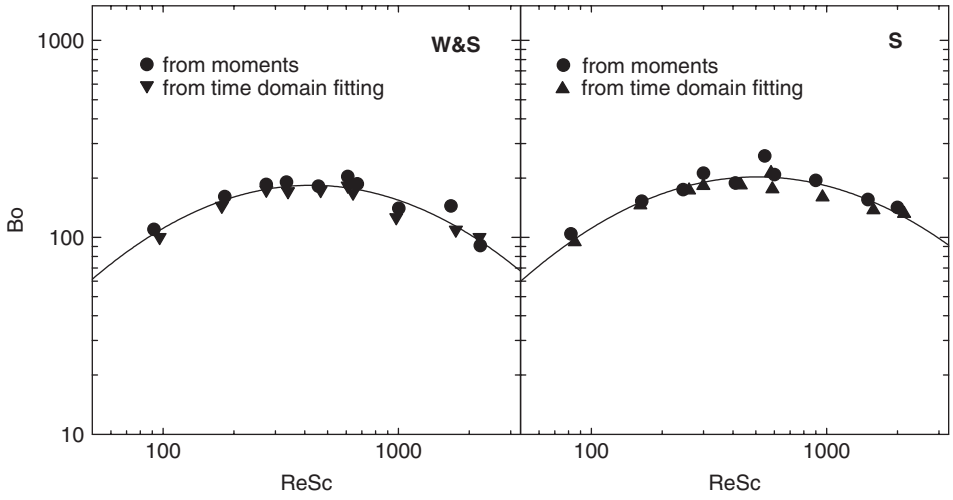

Fig. 6. Bo versus *ReSc* from second moments and wet columns response fitting.

The obtained Peclet numbers are compared with the results from moment analysis in Fig. 6. As can be seen the results from both methods are in fair agreement. The dependence of *Pe* versus *ReSc* can be interpolated by empirical formulas

$$Pe = a \exp\left[-\frac{1}{2} \cdot \frac{\ln(ReSc/b)}{c}\right]^2. \tag{18}$$

For the washcoat on carrier ($W\&S$): $a = 183.886$, $b = 1.4456$, $c = 426.249$; for the ceramic support (S) : $a = 202.857$, $b = 1.4817$, $c = 507.483$.

4.2. Effective diffusion coefficients

Effective diffusion coefficients of both tracer–carrier pairs (D_{ArN_2}, D_{HeN_2}) in columns packed with $W\&S$ and S were extracted from the corresponding diffusion times, t_{diff}, obtained by time-domain fitting of the corresponding column responses. The convolution integral (8) was applied in all cases. Two ways for obtaining the diffusion times, t_{diff}, were used:

(i) Three parameter fitting: Parameters t_c, *Pe* and t_{diff} were fitted; parameters γ/β and δ_0 obtained independently (see above) were fixed.
(ii) Two parameter fitting: Parameters t_c and t_{diff} were fitted. Peclet numbers were fixed at values from (18) (for non-porous packing with pores blocked by Porofil liquid) and for parameters γ/β and δ_0 the independently obtained values (see above) were used.

The obtained effective diffusivities for both cases are summarized in Table 4.

4.3. Application of the Bosanquet formula

According to the Bosanquet formula the effective diffusion coefficient D_{TC} can be separated into terms, which characterize the contribution of Knudsen- and bulk-diffusion:

$$\frac{1}{D_{TC}} = \frac{1}{\langle r\rangle\psi K_T} + \frac{1}{\psi D^m_{TC}}. \tag{19}$$

Here $K_T = (\frac{2}{3})(8R_gT/M_T)^{1/2}$ with the tracer molecular weight, M_T, gas constant R_g and temperature T. D^m_{TC} is the binary bulk-diffusion coefficient of the pair T–C, $\langle r\rangle$ stands for the mean transport-pore radius (the main part of gas diffusion takes place though transport pores) and ψ represents the ratio of transport-pore porosity and tortuosity. Because effective diffusivities for two gas pairs (Ar–N_2 and He–N_2) are available, it is possible to determine $\langle r\rangle\psi$ and ψ for both the ceramic support particles (S) as well as for the washcoat-on-ceramics particles ($W\&S$) (see Table 4).

By application of the "resistances-in-series" model

$$\frac{\ell_{W\&S}}{(\langle r\rangle\psi)_{W\&S}} = \frac{\ell_S}{(\langle r\rangle\psi)_S} + \frac{\ell_W}{(\langle r\rangle\psi)_W},$$
$$\frac{\ell_{W\&S}}{(\psi)_{W\&S}} = \frac{\ell_S}{(\psi)_S} + \frac{\ell_W}{(\psi)_W}, \tag{20}$$

both $\langle r\rangle\psi$ and ψ parameters for the washcoat-on-ceramics particles ($W\&S$) can be separated into parameters which characterize the washcoat layer (W). Here ℓ_{WS}, ℓ_S and ℓ_W represent the estimated thicknesses of the combined washcoat–ceramics layer, the ceramics layer and the washcoat layer. The obtained values are shown also in Table 4.

Using these values together with Bosanquet formula it was possible to determine the contribution of Knudsen- and bulk-diffusion mechanism for the net diffusion transport of tracer gas in porous particles. These calculations showed that for $W\&S$ particles neither Knudsen nor molecular diffusion predominates. For ceramic support the contribution of Knudsen diffusion was negligible. These data are in a good agreement with PSD data (see Fig. 2). The obtained percentage values of Knudsen transport contribution to net diffusion transport are summarized in Table 5.

Table 4
Transport characteristics of packing particles

Method	Layer kind and thickness (μm)	Effective diffusivity (cm^2/s)		$\langle r\rangle\psi$ (nm)	ψ (dimensionless)	$\langle r\rangle$ (nm)
		$Ar–N_2$	$He–N_2$			
Two parameter fitting	$\ell_{WS} = 105$	0.0024	0.0083	2.52	0.019	132
	$\ell_S = 70$	0.0077	0.0277	86.4	0.040	2136
	$\ell_W = 35$	0.0010	0.0034	0.86	0.009	92
Three parameter fitting	$\ell_{WS} = 105$	0.0056	0.0192	5.43	0.049	111
	$\ell_S = 70$	0.0068	0.0246	77.14	0.037	2067
	$\ell_W = 35$	0.0041	0.0133	1.9	0.125	15

Table 5
Percentage of Knudsen transport from net diffusion transport

Three-parameters fitting	$Ar \rightarrow N_2$ (%)	$He \rightarrow N_2$ (%)
Washcoat on ceramics	36	39
Ceramics	3	4
Two-parameters fitting		
Washcoat on ceramics	33	36
Ceramics	3	4

Table 6
Comparison of effective diffusion coefficient (290 K, 106 kPa m^2/s)

Ceramic support	$CO \rightarrow N_2$	$CH_4 \rightarrow N_2$
Zhang, Hayes and Kolaczkowski	0.97×10^{-6}	0.92×10^{-6}
This work: two parameter fitting[a]	0.82×10^{-6}	0.86×10^{-6}
This work: three parameter fitting[a]	0.75×10^{-6}	0.79×10^{-6}

[a]Calculated from transport parameters of Table 4 and (19).

Table 7
Calculated values of effective diffusivities (296 K, 101 kPa, 10^6 m^2/s)

	$C_3H_6 \rightarrow N_2$	$CO \rightarrow N_2$	$CH_4 \rightarrow N_2$
Blank washcoat (W)	0.075	0.113	0.130
Washcoat on ceramic support ($W\&S$)	0.171	0.266	0.299

Calculated for transport parameters and two parameter fitting of Table 4 and (19).

Finally, the transport parameters were used for calculations of effective diffusion coefficients for different pairs $T \rightarrow C$, particularly for pairs $CO–N_2$ and $CH_4–N_2$. The data obtained for ceramic support were compared with values published in literature. The cordierite, used as ceramic support, studied in this paper has nearly the same porous structure as one on which Kolaczkowski (2000) and Zhang et al. (2004) have measured their diffusion data. Comparison between the values obtained from the literature (Kolaczkowski, 2000; Zhang et al., 2004) and the values evaluated by using Bosanquet formula is shown in Table 6. It is clearly seen that for the two parameter fitting method the agreement between these cases is excellent, for the three parameter fitting method the agreement is worse, but still in the limits given by the authors.

Calculated values of effective diffusivities for different pairs $T \rightarrow C$, for both blank washcoat layer and washcoat on ceramic support, are shown in Table 7.

5. Conclusions

The chromatographic technique that employs SPSC and takes, via convolution, into account the extra-column effects of the measuring system could provide consistent transport characteristics of porous solids. These characteristics are material parameters of porous solid and, hence, independent of the nature of gases that are transported through pores, as well as of temperature and pressure. Transport parameters can be used, for evaluating effective diffusion coefficients for any $T \rightarrow C$ pairs.

Two approaches were tested for transport parameter evaluation:

(a) simultaneous fitting of three parameters: t_c, Pe, t_{diff},
(b) fitting of two parameters, t_c, t_{diff}, and use of Pe numbers determined separately with non-porous (liquid blocked) packing particles.

The second approach significantly improves the confidence of obtained pore-diffusion characteristics (effective diffusion coefficients).

True densities of $W\&S$ samples cut from different positions around the monolith perimeter vary more than 10%. The chromatographic technique suppresses this problem since the results are averaged over many pellets (more than 200 pellets were packed in columns).

The obtained transport characteristics could be used for estimation of effective diffusion coefficients for $CO–N_2$, $CH_4–N_2$ and $C_3H_6–N_2$ pairs, which are of interest world-wide. Such coefficients are only rarely found in the literature.

Notation

A	cross-sectional area
$c(x,t)$	interparticle tracer concentration
$c_0(t)$	shape of the tracer concentration pulse
$C(x,s)$	Laplace transform of interparticle tracer concentration

D_{TC}	effective diffusion coefficient for pair $T \rightarrow C$
D^m_{TC}	binary bulk diffusion coefficient for pair $T \rightarrow C$
E	axial dispersion coefficient
F	carrier-gas flow rate
K	dimensionless adsorption equilibrium constant for tracer gas
K_T	Knudsen diffusivity
ℓ	half-thickness of the layer
L	column length
M	molecular weight
$N(r)$	molar diffusion flux density per unit total cross-section of porous particles
Pe	Peclet number: $Pe = vL/E$
Q	Tortuosity
$\langle r \rangle$	mean radius of the transport pore
R	particle length coordinate ($r = 0$ at particle center,$r = \ell$ at particle outer surface)
R_g	universal gas constant
t_C	mean residence time of the tracer gas in SPSC
t_{diff}	diffusion time of the tracer in the pore structure of the particle
T	Temperature
$u(x, r, t)$	intraparticle tracer gas concentration
$U(x, r, s)$	Laplace transform of intraparticle tracer concentration
V	carrier-gas linear velocity
$w(x, r, t)$	concentration of adsorbed tracer
X	dimensionless column length coordinate

Greek letters

α	interparticle column void fraction
β	particle porosity
γ	pore volume per interstitial volume
δ_0	adsorptionparameter
ε_T	transport pore porosity
μ'_1	first absolute moment of the response peak
μ_2	second central moment of the response peak
ρ	particle density
ψ	transport parameter—ratio of transport pore porosity and tortuosity

Subscripts

$W\&S$	for washcoat layer on ceramic support
S	for ceramic support
W	for washcoat layer
C	carrier gas
T	tracer gas
I	for long column
II	for short column

Acknowledgments

The financial support of Grant Agency of the Czech Academy of Sciences (# A 4072404) and Grant Agency of the Czech Republic (GA 104/05/2616) is gratefully acknowledged.

References

Beeckman, J.W., 1991. Measurement of the effective diffusion coefficient of nitrogen monoxide through porous monolith-type ceramic catalysts. Industrial and Engineering Chemistry Research 30, 428–430.

Cybulski, A., Moujin, J.A., 1998. The present and the future of structured catalysts. In: Cybulski, A., Moujin, J.A. (Eds.), Structured Catalysts and Reactors. Marcel Dekker, New York, pp. 1–14.

Fahim, M.A., Wakao, N., 1982. Parameter estimation from tracer response measurements. Journal of Chemical Engineering Japan 25, 1–8.

Guasguo, Y., et al., 2000. The measurement of effective diffusivity for sulfur tolerant methanation catalyst. Chemical Engineering Journal 18, 141–146.

Gulati, S.T., 1998. Ceramic catalyst supports for gasoline fuel. In: Cybulski, A., Moujin, J.A. (Eds.), Structured Catalysts and Reactors. Marcel Dekker, New York, pp. 15–58.

Haynes, H.W., 1988. The experimental evaluation of catalyst effective diffusivity. Catalysis Review-Science and Engineering 30, 363–627.

Heck, R.M., Farrauto, R.J., 1995. Catalytic Air Pollution Control: Commercial Technology. Van Nostrand Reinhold, New York, pp. 11–26.

Himmelblau, D.M., Bischoff, K.B., 1968. Process Analysis and Simulation. Deterministic Systems. Wiley, New York.

Honig, G., Hirdes, U., 1984. A method for the numerical inversion of Laplace transforms. Journal of Computers and Applied Mathematics 10, 113–132.

Kašpar, J., et al., 2003. Automotive catalytic converters: current status and some perspectives. Catalysis Today 77, 419–449.

Koèí, P., et al., 2004. Modeling of three-way-catalyst monolith converters with microkinetics and diffusion in the washcoat. Industrial and Engineering Chemistry Research 43, 4503–4510.

Kolaczkowski, S.T., 2000. Evaluating the effective diffusivity of methane in the washcoat of a honeycomb monolith. Applied Catalysis 25, 93–104.

Kolaczkowski, S.T., 2003. Measurement of effective diffusivity in catalyst coated monoliths. Catalysis Today 83, 85–95.

Kubín, M., 1965. Beitrag zur Theorie der Chromatographie. Collection of Czechoslovak Chemical Communications 30, 1104–1118.

Kučera, E., 1965. Contribution of the theory of chromatography: linear non-equilibrium elution chromatography. Journal of Chromatography 19, 23–248.

Leung, D., et al., 1996. Diffusion limitation effects in the washcoat of a catalytic monolith reactor. Canadian Journal of Chemical Engineering 74, 94–103.

Mukadi, L.S., Hayes, R.E., 2002. Modeling the three-way catalytic converter with mechanistic kinetics using Newton–Krylov method on a parallel computer. Computers and Chemical Engineering 26, 439–455.

Press, W.H., Flannery, B.P., Teukolsky, S.A., Vetterling, W.T., 1986. Numerical Recipes. Cambridge University Press, Cambridge.

Ramathan, K., et al., 2003. Light-off criterion and transient analysis of catalytic monoliths. Chemical Engineering Science 58, 1381–1405.

Schneider, P., 1984. Time-domain expression for impulse response (chromatographic) curve for the Kubín–Kučera model of adsorption column. Chemical Engineering Science 39, 927–929.

Schneider, P., Smith, J.M., 1968a. Chromatographic study of surface diffusion. A.I.Ch.E. Journal 14, 886–895.

Schneider, P., Smith, J.M., 1968b. Adsorption rate constants from chromatography. A.I.Ch.E. Journal 14, 762–771.

Scott, D.S., et al., 1974. The measurement of transport coefficients in gas-solid heterogeneous reactions. Chemical Engineering Science 29, 2155–2167.

Seidel-Morgenstern, A., 1991. Analysis of boundary conditions in the axial dispersion model by application of numerical Laplace inversion. Chemical Engineering Science 46 (10), 2567–2571.

Šolcová, O., Schneider, P., 1996. Extra-column effects in determination of rate parameters by the chromatographic method. Collection of Czechoslovak Chemical Communications 61, 844–855.

Šolcová, O., Schneider, P., 2004. Axial dispersion in single pellet-string columns with non-porous packing. Chemical Engineering Science 59, 1301–1307.

Šolcová, O., et al., 1997. Determination of effective diffusivities and transport parameters of porous solids in the single-pellet-string-column. Catalysis Today 38, 71–77.

Šolcová, O., et al., 2006. Diffusion coefficients and other transport characteristics of specially shaped porous materials from chromatographic measurements. Microporous and Mesoporous Materials 91 (1–3), 100–106.

Twigg, M.V., Wilkins, A.J.J., 1998. Autocatalysts—past, present and future. In: Cybulski, A., Moujin, J.A. (Eds.), Structured Catalysts and Reactors. Marcel Dekker, New York, pp. 91–120.

Wakao, N., et al., 1979. Parameter estimation in adsorption chromatography by real-time analysis. Journal of Chemical Engineering Japan 12, 481–483.

West, D.H., et al., 2003. Experimental and theoretical investigation of the mass transfer controlled regime in catalytic monoliths. Catalysis Today 88, 3–16.

Zhang, F., et al., 2004. A new technique to measure the effective diffusivity in catalytic monolith washcoat. Chemical Engineering Research and Design 82 (A4), 481–489.